Composition optimization of Al-Zn-Mg-Cu alloy via thermodynamic calculation

Y. LIU*, D. M. JIANG, W. J. LI
School of Materials Science and Engineering, Harbin Institute of Technology, Harbin 150001, China

Phase fraction and solidification path of Al-Zn-Mg-Cu series aluminum alloy were calculated by thermodynamic calculation software Jmat-Pro. The variation of $MgZn_2$ and $A1_2CuMg$ phases and crystallization temperatures with Zn, Mg and Cu contents were studied in details. The thermodynamic calculation results indicated that, in the mass fraction ranges of Zn of 6.2-6.6%, Mg of 2.3%-2.5%, Cu of 1.9-2.1%, the content of $MgZn_2$ phase can be up to more than 4.5% and that of Al_2CuMg phase can be lower than 0.6% during the composition optimization of 7050 alloy.

(Received July 13, 2015; accepted September 29, 2016)

Keywords: A1-Zn-Mg-Cu alloy, Thermodynamic calculation, Composition optimization

1. Introduction

7xxx series alloys have been extensively used in automobile and aerospace structures and many other high strength structural components due to their excellent mechanical properties, high thermal and electrical conductivity, and superior resistance to corrosion [1-5]. Meanwhile, the performance can be further improved by constituent optimization and heat treatment. The development of Al-Zn-Mg-Cu alloys is closely related to the alloy composition optimization. Since the development of 7075 alloy in 1943, a series of comprehensive performance of ultra-high-strength aluminum alloys are developed by adjusting the contents of main alloying elements (Zn, Mg, Cu), adding trace elements (Cr, Zr, Sc) and reducing impurity element contents (Fe, Si), such as 7050,7150,7055 and 7085 alloy[6-8]. It is known that different contents of Zn, Mg and Cu will play an important role in the formation of $\eta(MgZn_2)$, $T(Al_2Mg_3Zn_3)$, $S(Al_2CuMg)$ and $\theta(Al_2Cu)$ phases, which will influence performances of the precipitation hardenable Al-Zn-Mg-Cu alloys [7].

Generally, the increase of Zn and/or Mg content has a significant effect on the formation of the major strengthening phases (e.g., GP zone, η' and η phases), and undoubtedly will enhance the strength of the Al-Zn-Mg-Cu series alloys[9]. However, Al-Zn-Mg-Cu alloys with high Zn and Mg content usually exhibit lower fracture toughness and corrosion performances, due to the insufficient dissolution of the existence of lots of coarse intermetallic particles during homogenization and solution treatment[10-12]. It has been shown that the addition of Cu can improve the stress-induced corrosion cracking sensitivity and has a significant effect on the aging behaviors of Al–Zn–Mg alloys, such as the acceleration of the precipitation kinetics from GP zones to η' phase, stabilize the η' phase from changing into η phase [13-18]. However, whether Cu modifies the existing aging process and introduces additional precipitates is still uncertain [13].

Generally, "trial and error" mode was used as the main approach for materials scientists to understand the kinds and amount of these phases. Therefore, long development cycle and high research cost have to be needed, which cannot meet the needs of rapid development of aluminum alloy [7,8]. Recently, the solidification simulation technology, such as calculation of phase diagram (CALPHAD) method, has been partially replaced the "trial and error" mode applied in traditional materials development with reducing product development time, which can optimize the alloy properties and forecast alloy microstructure and micro segregation. Thermo-Calc, Thermosuite, Jmat-Pro, MTDATA, FACT and PANDAT are the typical calculation of phase diagram (CALPHAD) software[19,20]. Several researchers assessed formation of phases in multicomponent aluminum alloys, providing support for alloy designation[21-30]. This work is focused on the application of the calculation of phase diagrams method for alloy composition designation. In our present study, we analyzed the effects of main alloying elements on phase fraction and crystallization temperature in Al-Zn-Mg-Cu alloy.

2. Calculation principle and experiment procedure

2.1. Thermodynamic principle of CALPHAD

Currently, calculation of phase diagram (CALPHAD) method gradually enters in a new stage of thermo-chemical

and computational research from experimental determination of the equilibrium phase diagram, which contains the most widely used method of thermodynamic phase diagram and kinetics of phase transformation method i.e. CALPHAD[19,20]. CALPHAD technology is a research system covering thermodynamic properties, phase equilibrium data, the experimental phase diagram data, crystal structure, magnetic, and other order-disorder transition information as a whole, which describes each phase thermodynamic data and the corresponding Gibbs free energy expression. Thermodynamics essence of phase diagram is to obtain the relationship between the target system and alloy composition to get the content of each constituent under isothermal and isobaric conditions [7,31].

According to thermodynamic principles, under constant temperature and pressure conditions, the general conditions of thermodynamic equilibrium system is the minimum Gibbs free energy of the target system.

$$G = \sum_{i=1}^{C} f^i G_m^i = \min \qquad (i=1,\ldots,C) \qquad (1)$$

where G is the Gibbs free energy of the target system; f is the molar fraction of the i phase; the total phase number is C; G_m^i is the partial Gibbs free energy of the i phase.

Based on the rule of the minimum Gibbs free energy, we can deduce the rule of equal chemical potential of each phase:

$$\mu_i^{(1)} = \mu_i^{(2)} = \mu_i^{(3)} = \cdots = \mu_i^{(C)} \qquad (i=1,\ldots,C) \qquad (2)$$

where C is the number of equilibrium phase in the target system.

Thermodynamic model should be selected based on the physical and chemical properties of the phase and reflect the physical parameters of the target system, which is the basis for calculation and optimization of phase diagrams.

2.2. Materials and thermodynamic model

The compositions of materials calculated were based on Al-5.85Zn-2.28Mg-2.13Cu alloy. The contents of Zn, Mg and Cu were in the ranges of 5.8%~6.6%, 2.1%~2.5% and 1.9%~2.3%, respectively. All of the calculations were processed by thermodynamic calculation software Jmat-Pro. Solidification paths of Al-5.85Zn-2.28Mg-2.13Cu alloy were calculated using Scheil model (non-equilibrium model). The contents and crystallization temperatures of η(MgZn2) and S(Al2CuMg) phases existing in Al-Zn-Mg-Cu alloys were calculated.

2.3. Experiment procedure

The material used in this study was rolled 7050 45 mm thick plate (5.85 Zn, 2.28 Mg, 2.13 Cu, 0.094 Zr, 0.055 Fe, 0.019 Mn, 0.041 Si and balance Al, in wt.%), provided by Northeast Light Alloy Co., Ltd.. Differential scanning calorimetry (DSC) was carried on the sample using a DSC Q2000 V24.9 Build 121 instrument. The sample for DSC analysis was punched into small disc with thickness of 1 mm and a diameter of 4 mm. The quality of the specimen was smaller than 30mg. The specimen was submitted to DSC under a Nitrogen atmosphere with scanning rates of 10K/min.

3. Results and discussion

3.1. Thermodynamic calculation for solidification paths

Fig. 1 showed the curves of solid fraction changing with temperatures. In non-equilibrium curve, α(Al) began to precipitate at 633.41 °C. And the non-equilibrium transformation temperature of S(Al_2CuMg) phase and η($MgZn_2$) were 482.15 and 475.41°C, respectively. The solidus temperature was 468°C for non-equilibrium solidification. With the decrease of solidification temperature, Al_3Zr, α(Al), Al_3Fe, Al_2CuMg, Al_7Cu_2Fe, Mg_2Si and η($MgZn_2$) phases were gradually generated in the non-equilibrium solidification process.

Fig. 2 showed the DSC curve of Al-5.85Zn-2.28Mg-2.13Cu alloy. There was an obvious exothermic peak at 478.64 °C corresponding to dissolution of low melting point eutectic phase. The peak temperature was consistent with the temperature calculated by non-equilibrium model. This melting temperature can be used as an important reference temperature to determine the solution heat treatment procedures.

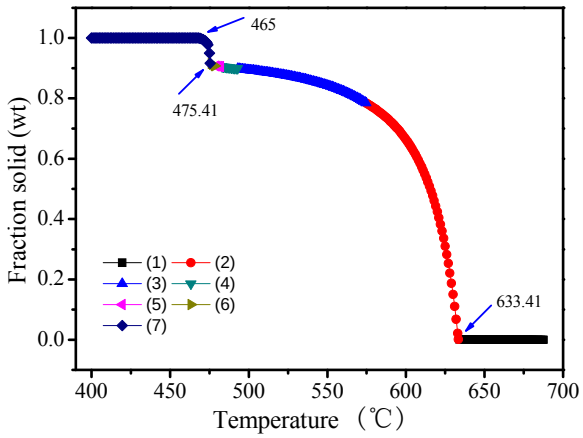

Fig.1. Solidification paths of Al-5.85Zn-2.28Mg-2.13Cu alloy by thermodynamic calculation 1—L + Al_3Zr (687.65-633.41) 2—L + Al_3Zr + α(Al) (633.41-574.67) 3—L + Al_3Zr + α(Al) + Al_3Fe (574.67-492.88) 4—L + Al_3Zr + α(Al) + Al_3Fe+Mg_2Si (492.88-482.15) 5—L + Al_3Zr + α(Al)+ Al_3Fe+Mg_2Si+Al_7Cu_2Fe (482.15- 478.42) 6—L + Al_3Zr + α(Al) + Al_3Fe + Mg_2Si + Al_7Cu_2Fe + Al_2CuMg(478.42-475.41) 7—L + Al_3Zr + α(Al) + Al_3Fe + Mg_2Si + Al_7Cu_2Fe+Al_2CuMg+η($MgZn_2$) (475.41-400)

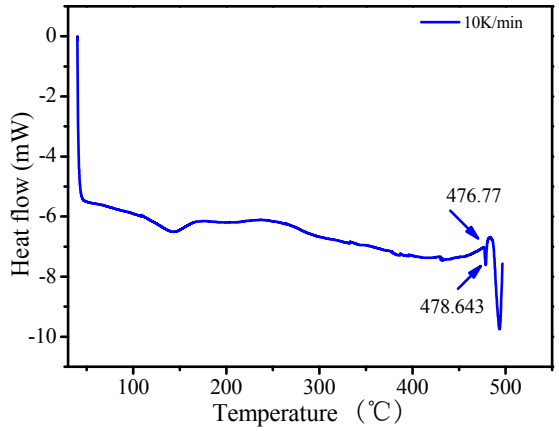

Fig. 2. DSC curve of Al-5.85Zn-2.28Mg-2.13Cu alloy

3.2 Phases in calculated alloys

In order to further investigate the detail of $\eta(MgZn_2)$, $\theta(Al_2Cu)$ and $S(Al_2CuMg)$ phases in Al-Zn-Mg-Cu alloy, mass fraction of each phase was calculated. In our calculated alloys, $\eta(MgZn_2)$ was the main precipitation and $S(Al_2CuMg)$ phase existed as intermetallic phase. While Al-xZn-2.1Mg-2.3Cu alloy with the compositions of Zn were in the ranges of 6.2%~6.6%, $\theta(Al_2Cu)$ phase appeared in these calculated alloys. The amount of θ(Al2Cu) increased as the content of Zn increased, as shown in Fig.3. For other calculated alloys only η(MgZn2) and θ(Al2Cu) phases were considered.

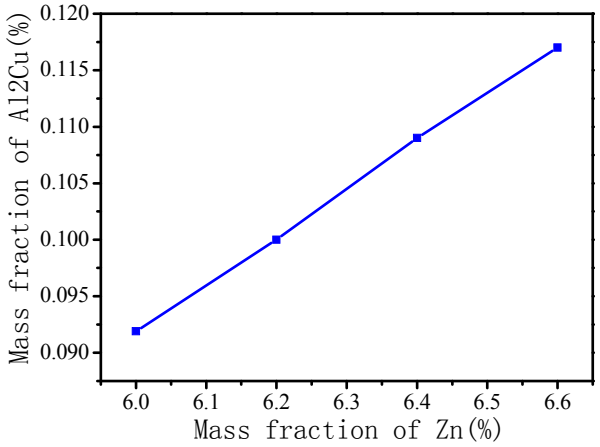

Fig. 3. Variation of Al2Cu phase amount in Al-xZn-2.1Mg-2.3Cu alloy with Zn content

Fig. 4 showed the variation of $MgZn_2$ crystallization temperature and phase amount with Zn content. The $\eta(MgZn_2)$ crystallization temperature was in the range of 473.5~476 °C and the more Mg contents, the higher $\eta(MgZn_2)$ crystallization temperature. As the Cu and Zn contents increased, $\eta(MgZn_2)$ crystallization temperature experienced a decrease trend. Meanwhile, the amount of $\eta(MgZn_2)$ phase exhibited a gradually increase with the increase of Zn and Mg contents and a decrease with the increase of Cu contents.

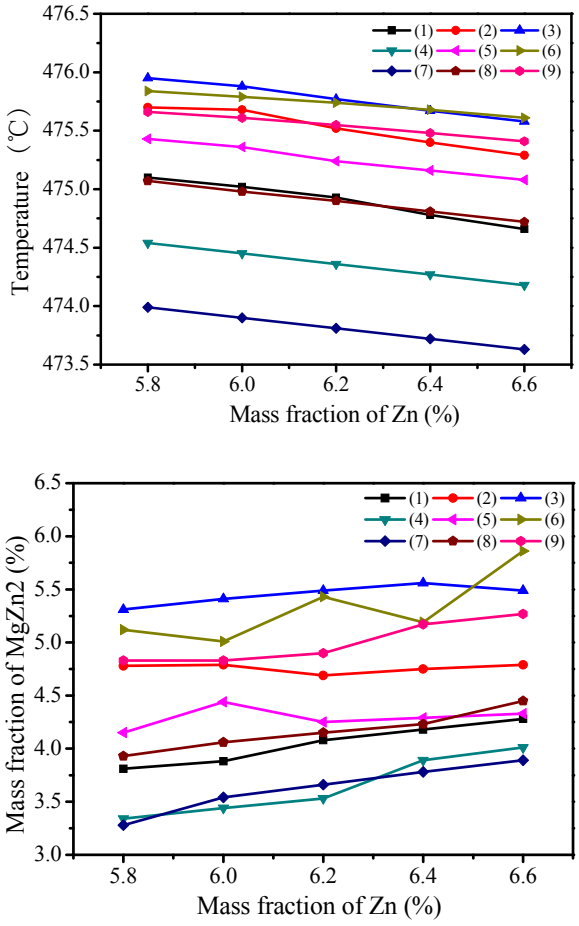

Fig. 4. Variation of $MgZn_2$ crystallization temperature (a)and phase amount (b)with Zn content
(1) 2.1Mg-1.9Cu (2) 2.3Mg-1.9Cu(3) 2.5Mg-1.9Cu
(4) 2.1Mg-2.1Cu (5) 2.3Mg-2.1Cu (6) 2.5Mg-2.1Cu
(7) 2.1Mg-2.3Cu (8) 2.3Mg-2.3Cu (9) 2.5Mg-2.3Cu

Fig.5 showed the variation of Al_2CuMg crystallization temperature and phase amount with Zn content. The $S(Al_2CuMg)$ crystallization temperature was in the range of 471-481°C and the more Zn contents, the lower $S(Al_2CuMg)$ crystallization temperature. As the Cu contents increased, S(Al2CuMg) crystallization temperature experienced an increase trend. Meanwhile, the amount of S(Al2CuMg) phase exhibited a gradually decrease with the increase of Zn and Mg contents and an increase with the increase of Cu contents.

In order to obtain high strength, there must be a sufficient number of $\eta(MgZn_2)$ phase. Although $S(Al_2CuMg)$ phase can play a strengthening effect, their insufficient dissolution during the subsequent homogenization and solution process will result in a significantly lower alloy plasticity and toughness. Due to the small amount of $\theta(Al_2Cu)$ phase, the strengthening effect was limited. Therefore, the increase of $\eta(MgZn_2)$ phase and decrease of $S(Al_2CuMg)$ will make alloys obtain

excellent mechanical properties. The alloys with contents of Zn, Mg and Cu in the ranges of 6.2% ~ 6.6%, 2.3% ~ 2.5% and 1.9%~2.1% will obtain more than 4.5% $\eta(MgZn_2)$ phase and less than 0.6% $S(Al_2CuMg)$ phase.

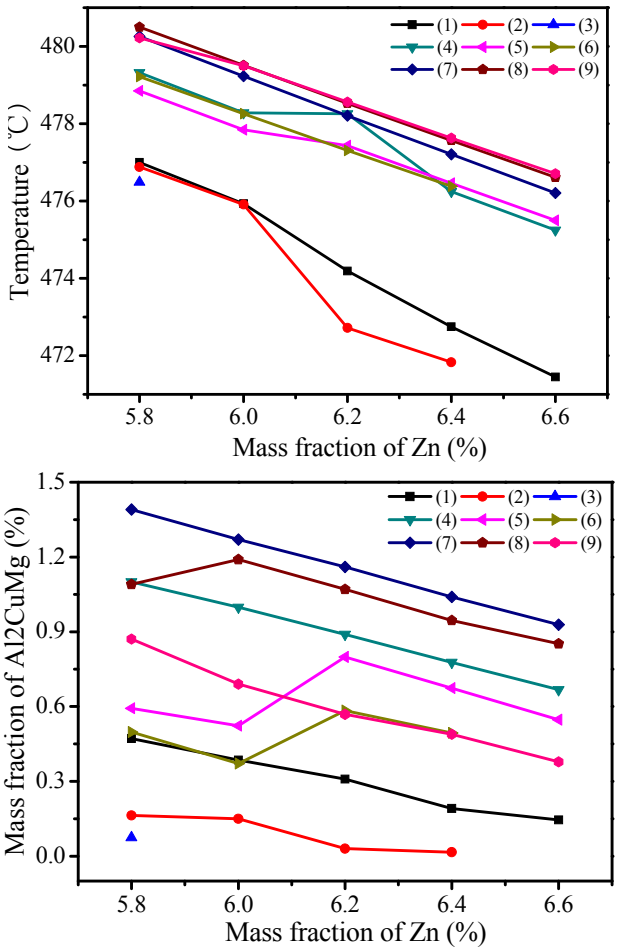

Fig.5 Variation of $A1_2CuMg$ crystallization temperature (a)and phase amount (b)with Zn content

(1) 2.1Mg-1.9Cu (2) 2.3Mg-1.9Cu(3) 2.5Mg-1.9Cu

(4) 2.1Mg-2.1Cu (5) 2.3Mg-2.1Cu (6) 2.5Mg-2.1Cu

(7) 2.1Mg-2.3Cu (8) 2.3Mg-2.3Cu (9) 2.5Mg-2.3Cu

4. Conclusions

CALPHAD method had been applied to thermodynamic calculation for Al-5.85Zn-2.28Mg-2.13Cu alloy. With the decrease of solidification temperature, Al_3Zr, α(Al), Al_3Fe, Al_2CuMg, Al_7Cu2Fe, Mg_2Si and $\eta(MgZn_2)$ phases were gradually generated in the non-equilibrium solidification process. The $\eta(MgZn_2)$ crystallization temperature was in the range of 473.5~476℃. Increasing Mg content or decreasing Cu and Zn contents can elevate the $\eta(MgZn_2)$ crystallization temperature. The $S(Al_2CuMg)$ crystallization temperature was in the range of 471~481℃. Increasing Cu content or decreasing Zn content can elevate the $S(Al_2CuMg)$ crystallization temperature. As the Zn and Mg contents increased, the amount of $\eta(MgZn_2)$ phases increased while the amount of $S(Al_2CuMg)$ phase decreased. High Cu content will induce high fraction of $S(Al_2CuMg)$ phase and had an adverse influence on $\eta(MgZn_2)$ phase. The alloys with contents of Zn, Mg and Cu in the ranges of 6.2%~6.6%, 2.3%~2.5% and 1.9%~2.1% will obtain more than 4.5% $\eta(MgZn_2)$ phase and less than 0.6% $S(Al_2CuMg)$ phase.

References

[1] J. P. Immarigon, R. T. Holt, A. K. Koul, L. Zhao, W. Wallace, C. Beddoes, J. Mater. Charact. **35**, 41 (1995).
[2] J. C. Williams, E. A. Starke Acta Mater. **51,** 5775 (2003).
[3] A. Heinz, A. Haszler, C. Keidel, S. Moldenhauer, R. Benedictus, W. S. Miller Mat Sci Eng A. **280,** 102 (2000).
[4] W. S. Miller, L. Zhuang, J. Bottema, A. J. Wittebrood, P. De Smet, A. Haszler, A. Vieregge Mat Sci Eng A. **280,** 37 (2000).
[5] B. Liu, C. Q. Peng, R. C. Wang, X. F. Wang, T. T. Li, Trans. Nonferrous Mat. Soc. China **20**, 1705 (2010).
[6] E. T. George, D. M. Scott, Handbook of aluminum: Physical metallurgy and processes [M]. New York: Marcel Dekker, Inc., 185 (2003).
[7] J. T. Liu, Y. A. Zhang, X. W. Li, Z. H. Li, B. Q. Xiong, J. S. Zhang, Trans. Nonferrous Met. Soc. China **24,** 1481 (2014).
[8] Y. Han, L Li, Z. Z. Deng, Y. K. Le, X. M. Zhang, Trans. Nonferrous Met. Soc. China. **21**, 179 (2011).
[9] W. X. Shu, L. G. Hou, J. C. Liu, C. Zhang, F. Zhang, J. T. Liu, L. Z. Zhuang, J. S. Zhang, Metall. Mater. Trans. A **46,** 5375 (2015).
[10] D. Dumont, A. Deschamps, Y. Brechet, Mater. Sci. Eng. A. **356**, 326 (2003).
[11] Y. Deng, Z. M. Yin, F. G. Cong, Intermetallics. **26**, 114 (2012).
[12] D. K Xu, N. Birbilis, D. Lashansky, P. A. Rometsch, B. Muddle C: Corros. Sci., **53**, 217 (2011).
[13] X. Fang, Y. Du, M. Song, K. Li, C. Jiang, J. Mater. Sci. **47**, 8174 (2012).
[14] I. Polmear, J. Inst Metals **89**, 51 (1960).
[15] J. T. Staley, In: Vasudervan A. K. Doherty, R. D. (eds) Treatises in materials science and technology, Academic Press, New York. 31 (1988).
[16] S. K. Maloney, L. J. Polmear, S. P. Ringer, Mater. Sci. Forum. **1055**, 331 (2000).
[17] N. Q. Chinh, J. Lendvai, D. H. Ping, K. Hono, J. Alloys. Compd. **378**, 52 (2004).
[18] L. Hadjadj, R. Amira J. Alloys. Compd. **484**, 891 (2009).
[19] F. Y. Chen, W. Q. Jie, Acta Metallurgica sinica. **40**, 664 (2004).

[20] Z. H Dai, J. T. Lu, G. Kong, Mater. Review **20**, 94 (2006).
[21] A. R. Farkoosh, M. Javidani, M. Hoseini, D. Larouche, M. Pekguleryuz J. Alloys. Compd. **55**, 596 (2013).
[22] J. He, Journal of Northeastern University. **31,** 245 (2010) (in Chinese).
[23] H. X. Liu, C. P. Wang, Y. Yu, X. J. Liu, Y. Takaku, I. Ohnuma, R. Kalnuma, K. Ishida, J. Phase Equilib. Diff. **33,** 9 (2012).
[24] B. Hallstedt, Use of calphad thermodynamics to simulate phase formation during semi-solid processing [C]// Proceedings of the Semi-Solid Processing of Alloys and Composites. Aachen, Germany: Trans Tech Publications Ltd, 2008, 641.
[25] D. Mirkovic, J. Gröbner, R. Schmid-Fetzer, Acta Mater. **56,** 5214 (2008).
[26] Z. He, H. B. Zhou, Z. Y. Zhang, L. Y. Li, Adv. Mater. Res. **49**, 396 (2012).
[27] W. G. Zhao, X. C. Ye, W. J. Liu, M. C. Gu, Adv. Mater. Res. **503**, (3742012).
[28] J. J. Yu, X. M. Li, J. Phase Equilib. Diff. **32**, 350 (2011).
[29] J. J. Yu, X. M. Li, X. Q. Yu, Journal of Shanghai Jiao Tong University: Science. **17**, 286 (2012).
[30] J. Grobner, L. L. Rokhlin, T. V. Dobatkina, R. Schmid-Fetzer, J. Alloys. Compd. **433**, 108 (2007).
[31] N. Saunders, A. P. Miodownik, CALPHAD (Calculation of phase diagrams): A comprehensive guide [M]. New York: Pergamon Press, 1998, 47.

*Corresponding author: ly520208@163.com